



Study on Seismic Performance of Precast Hollow Slab Vertical Wall Based on Steel Plate Connection

Yi Wang^{1,2*}, Yansong Li², Xingtao Zeng¹, Chengcheng Guo²

¹ School of Civil and Transportation Engineering, Henan Urban Construction College, Pingdingshan, China

² College of Civil Engineering and Architecture, Three Gorges University, Yichang, China

*E-mail: wangy@huuc.edu.cn

Abstract. Since the reform and opening up, the national economy has experienced unprecedented development; however, along with the rapid economic development, the environmental and sustainable development problems behind it have become more and more prominent. Compared with the assembled reinforced concrete structure, prefabricated hollow core slabs, due to its mechanical properties superior to cast-in-place solid concrete, acoustic insulation and thermal insulation capabilities, and as a very common horizontal force components and is widely used, while in the multi-storey residential buildings, the use of prefabricated hollow core slabs also effectively reduces the structural dead weight, effectively improving the overall seismic performance of the structure. The objective of this study is to investigate the seismic performance of prefabricated hollow core slabs used as walls and to propose a nodal connection method for assembled hollow core slab walls composed of prefabricated hollow core slabs when placed vertically. The finite element models of the assembled hollow core slab wall and the conventional hollow core slab wall with the proposed nodal connection method are constructed using the finite element software ABAQUS and numerical simulations are carried out. The feasibility and reliability of the nodal connection method are verified by comparing and analysing the hysteresis curve, ductility curve and stiffness degradation curve of the two. The results show that the proposed connection is an effective solution with good seismic and structural performance. These results provide a useful reference for the practical application of prefabricated hollow core slabs with vertical wall structures, and are expected to promote research and development in related fields.

Keywords: assembled buildings; prefabricated hollow core slabs; joint node design; numerical simulation; mechanical property study

1 Introduction

The prefabricated hollow wall^[1] has become increasingly popular due to its excellent insulation and heat resistance properties, as well as its labour saving, short construction time and environmental friendliness. However, research on this structure is still at

an early stage. Scholars at home and abroad have conducted extensive simulations and experiments [2-5] and concluded that the prefabricated hollow shear wall has good seismic performance, and the presence of the post-pouring belt and holes has little effect on the seismic performance of the structure. The seismic performance of the test specimens also meets current code requirements.

For the precast wall, if the connection design is improper, it may show poor performance and premature failure. Peiyun Luo [6] and other researchers proposed a new prefabricated shear wall system using prefabricated bidirectional hollow concrete panels. Through experiments on one cast-in-place concrete shear wall and four prefabricated bi-directional hollow panel shear walls, the results show that all specimens meet the requirement of "strong in bending and weak in shear".

Combining the above research results, we propose a new prefabricated hollow core panel vertical wall structure that is suitable for mass production in factories, and at the same time, its load-bearing capacity can meet the needs of low-rise farm houses. In addition, we are also proposing a new type of jointing method, which can solve the problems of weak bonding that may occur in the previous dry jointing method, and the problems of construction influence and environmental pollution that may occur in the wet jointing method. This type of joint is convenient for construction and can ensure the good bearing capacity of the whole structure.

2 Design of Connection Nodes for Vertical Hollow Core Slab Wall Structures

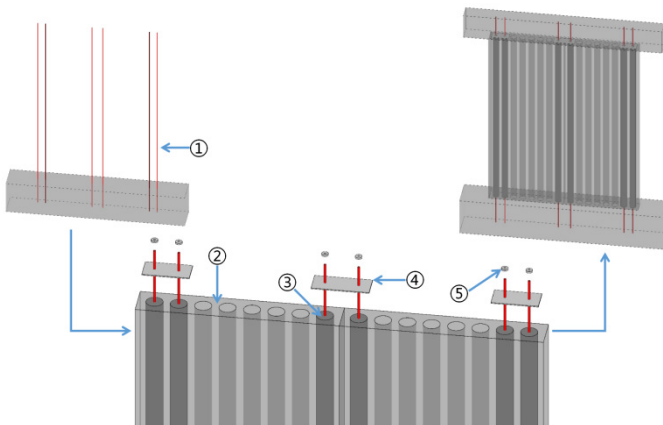


Fig. 1. Node design scheme. Annotation: ①-deformed bar connection through rib removing; ②-precast hollow slab; ③-grout concrete; ④-connecting steel plate; ⑤-nut

Figure 1 shows the construction of the nodal connection. The process begins by positioning and anchoring the perforated bars for a specific length in the foundation beam. Next, the corresponding holes in the hollow core slab are aligned with the perforated reinforcement, which are then calibrated to fit snugly into the holes. Next, the corre-

sponding holes in the hollow core slab are aligned with the perforated reinforcement, which are then calibrated to fit snugly into the holes. Concrete filling is then carried out for the perforated holes of the reinforcement bars, followed by the use of connection plates and bolts to establish connections between neighbouring perforated reinforcement.

Among them: Hollow slab wall is $3000\text{mm} \times 2400\text{mm} \times 200\text{mm}$, foundation beam is $3300\text{mm} \times 600\text{mm} \times 400\text{mm}$, loading beam is $3200\text{mm} \times 400\text{mm} \times 400\text{mm}$; longitudinal reinforcement within the hollow plate is symmetrically arranged, perforated steel bars were arranged in the two adjacent hollow plate nearest holes and holes in the edge of the wall, both of which are extended into the foundation beam 530mm , loading beam 380mm , hollow plate joints and the edge of the wall at the connection plate are $3000\text{mm} \times 2400\text{mm}$ thick are $t = 10\text{mm}$, structural drawings see Figure 2, the size of reinforcement and other selected standards [7].

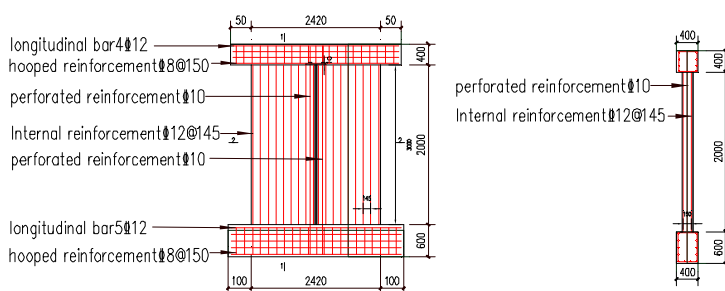


Fig. 2. Node connection wall structure diagram

3 Model Verification

3.1 Parameters of the Specimen

To verify the accuracy of the finite element parameters such as the concrete material intrinsic calculation method, the component indirect contact and boundary condition setting, and the loading method, two sets of hollow slab shear wall specimens WA4-2 and WC4-2 in the test described in the literature^[8] were selected as the verification model. Establishment of a finite element model with equivalent parameters.

The specific parameters are as follows: the overall height of the specimen used is 2090 mm, in which the section size of the loading beam is $420 \times 350\text{ mm}$ and the length is 1730 mm; the section size of the ground beam is $750 \times 650\text{ mm}$ and the length is 2600 mm.

3.2 Establishment of Finite Element Model

3.2.1 Mesh Size Determination and Cell Assignment.

When using the finite element software ABAQUS for numerical simulation, the two-dimensional point linear type (T3D2) in the three-dimensional truss element is

used ; concrete is defined as the eight-node linear reduced integral type (C3D8R) in the three-dimensional solid element. The concrete grid size is determined to be 50 mm, the concrete grid size of the loading beam and the foundation beam is 250 mm, and the steel grid size is 50 mm.

3.2.2 Material Constitutive Determination.

The calculation and determination of material constitutive relation have an important influence on the accuracy of numerical simulation results. ABAQUS has a tensile and compressive plastic damage model suitable for concrete structures. According to the design data of the relevant specimens in the literature [8] and the relevant provisions of the ' Code for Design of Concrete Structures ' (GB 50010-2010) , the uniaxial stress-strain relationship of concrete is shown in Table 1.

Table 1. Concrete parameters

| Specimen number | design value of compressive strength f_c (MPa) | Compressive strength test value f_{cu} (MPa) | tensile strength f_{tk} (MPa) | elastic modulus E_c ($\times 10^4$ MPa) | poisson ratio μ |
|-----------------|--|--|---------------------------------|--|---------------------|
| WA4-2 | 60 | 52.47 | 2.85 | 3.60 | 0.2 |
| WC4-2 | | 50.82 | | | |

At the same time, the stress-strain relationship of the steel bar adopts the double broken line model. According to the design data of the relevant specimens in the literature and the ' Code for design of steel structures ' GB50017-2017, the mechanical properties of the steel are shown in Table 2.

Table 2. Steel parameters

| steel reinforcement | Diameter (mm) | yield strength f_y (MPa) | tensile strength f_u (MPa) | Elongation (%) | elastic modulus ($\times 10^5$ MPa) | poisson ratio μ |
|---------------------|---------------|----------------------------|------------------------------|----------------|--------------------------------------|---------------------|
| HPB300 | 6 | 300 | 420 | | 2.10 | |
| HRB400 | 8 | 448 | 652 | 19 | 2.23 | 0.3 |
| | 10 | 458 | 666 | | 2.10 | |

2.2.3 Contact, Boundary Conditions and Loading Mode.

Considering the constraint effect of the built-in connection steel plate of the hollow slab wall on the surrounding concrete, when setting the contact between the steel and the concrete, the bond slip between the materials is ignored, and the steel plate is built into the concrete ; at the same time, the bond-slip effect between the bolt and the steel plate is neglected, and the connection between the two is considered to be intact. The other boundary conditions are consistent with the experimental boundary conditions. The bottom beam of the numerical model is set to be consolidated, and the upper loading beam is set to be a sliding support along the in-plane direction of the wall.

In the finite element solution, the load is applied in two steps. The first step is the vertical load, which is determined by the design axial pressure and acts on the central coupling point of the top surface of the loaded beam to simulate the constant and live load conditions of the structure under normal service conditions. The second part is the horizontal reciprocating load, whose amplitude is determined by the joint force-displacement control recommended by the ' Building Seismic Test Code ' JGJ / T101-2015, and acts on the cross section of the end of the loaded beam until the specimen yields.

3.3 Finite Element Model

In order to verify the rationality of the above parameters, the finite element models FEM-1 and FEM-2 corresponding to the specimens WA4-2 and WC4-2 in Reference^[7] were established respectively, and the loading test was carried out. The loading system is consistent with the test. The numerical simulation is compared with the experimental skeleton curve, as shown in Fig.3.

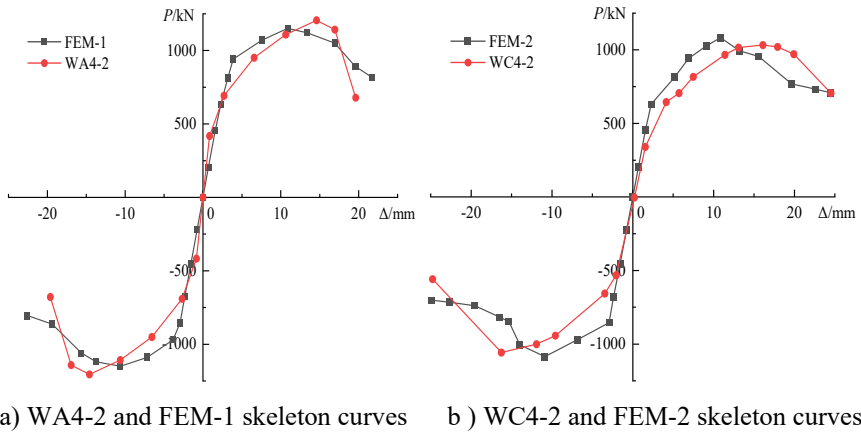


Fig. 3. Comparison of skeleton curves between test specimens and finite element specimens

From the (a) and (b) diagrams, it can be seen that the skeleton curves obtained from the test and finite element analysis are basically consistent. At the initial stage of loading, the slope of the two is basically constant, which indicates that the lateral stiffness of the specimen is basically unchanged at this stage. With the increase of load, the slope of the skeleton curve gradually decreases, indicating that the lateral stiffness of the specimen is degraded. The main reason is that the increase of load leads to the aggravation of concrete damage. The peak error of the skeleton curve obtained by the test and numerical simulation is less than 5 %, which meets the engineering accuracy requirements. Therefore, the two sets of hollow slab shear wall specimen models and parameter settings established by ABAQUS have good feasibility and accuracy.

4 Analysis of Bearing Capacity of Hollow Slab Wall

In order to analyze the bearing capacity of the vertical horizontal connection of the prefabricated hollow slab assembled wall, according to the above finite element modeling method, referring to the parameters such as the size and material properties of the above structure diagram, the horizontal connection prefabricated hollow slab assembled wall structure (number GCW-1) and the same size (no connection method The whole wallboard) prefabricated hollow slab assembled wall (number GCW-2) is shown in Figure 4. The vertical pressure of 2900 KN is applied at the top of the loading beam, and the axial compression ratio of the test is 0.3. The hysteresis curve, skeleton curve and ductility coefficient are obtained and compared and analyzed as follows.

The hysteresis performance is not only the main basis for studying the seismic performance of the specimen, but also the necessary basis for determining the restoring force model of the specimen. Fig.4 shows the hysteresis curves of GCW-1 and GCW-2.

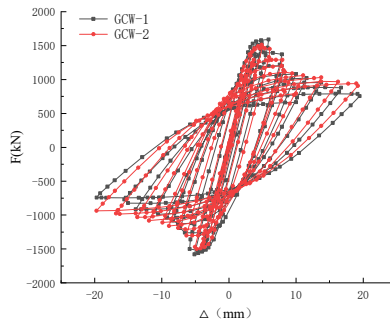


Fig. 4. Hysteresis curve

It can be seen from Fig.4 that GCW-1 and GCW-2 are fusiform, indicating that both have good plastic deformation ability, and the hysteresis curves of the two are basically consistent. Based on the observation results, it can be clearly observed that the two hysteresis loops have a relatively full shape, and there is a high characteristic consistency between them. There is no connection between the wallboards, which does not have a great impact and difference on the hysteresis performance of the two specimens.

The skeleton curve can directly reflect the change of the bearing capacity of the shear wall, which is the envelope of the hysteresis curve. Figure 5 is the comparison of the skeleton curves of the finite element model GCW-1 and GCW-2.

It can be concluded that the overall trend of the skeleton curves obtained by the two specimens is basically similar. The change of the connection mode between the wallboards of the specimens GCW-1 and GCW-2, and the difference of the early loading stiffness of the wall structure is not obvious. Because GXW-2 is a structure composed of a whole plate, the overall stiffness is large and the ultimate load is relatively high. The ultimate load of GCW-1 is relatively low. After the ultimate load, the stiffness of the specimen gradually decreases with the failure of the concrete. Due to the increase of

lateral displacement, the bearing capacity of GCW-2 decreases greatly due to the large stiffness and insufficient plastic deformation.

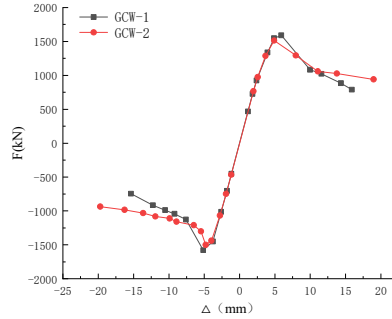


Fig. 5. Comparison of skeleton curves

Ductility performance is an important parameter index of wall structure, which reflects the plastic deformation ability of the whole structure. The yield point and limit point of the specimen are defined by Park method, as shown in Table 3. In this formu

Table 3. Ductility coefficient of hollow slab wall structure under different connection modes between wallboards

| Specimen number | direction | Δy (mm) | $\Delta \bar{y}$ (mm) | Δu (mm) | $\Delta \bar{u}$ (mm) | $\bar{\mu}$ |
|-----------------|-----------|-----------------|-----------------------|-----------------|-----------------------|-------------|
| GCW-1 | ortho | 3.89 | | 18.19 | | |
| | minus | 4.19 | 4.04 | 18.33 | 18.26 | 4.52 |
| | minus | 4.21 | | 18.97 | | |
| GCW-2 | ortho | 3.67 | | 17.88 | | |
| | minus | 4.05 | 3.86 | 18.24 | 18.06 | 4.68 |

Analysis of the data in Table 3 shows that the effect on the ductility coefficient of the wall structure of the hollow core slab is small under different inter-wallboard jointing methods; the trend of the ductility coefficient of the specimens during the change of the inter-wallboard jointing method has no obvious pattern, but all of them meet the requirements of the specification of not less than 3.0.

5 Conclusion and Foresight

After comparing the hysteresis curve, skeleton curve and ductility parameters of the same size wall, we found that both have excellent plastic deformation capability. Both hysteresis curves and skeleton curves show the same trend. Meanwhile, the ductility coefficients of the hollow core slab walls are less affected under different wall connection methods. In summary, the two specimens show good performance in terms of plastic deformation capacity and structural ductility. Therefore, it can be concluded

that this connection method is a feasible method and can effectively solve the problems of weak bond that may exist in the previous dry connection method, construction influence and environmental pollution in the wet connection method. This type of joint facilitates construction and also ensures the overall good load-bearing capacity of the structure.

The lack of transverse reinforcement in the assembled hollow core slab wall structure proposed in this paper results in slightly lower performance in terms of lateral stiffness, ductility coefficient and energy dissipation capacity parameters than that of the conventional assembled shear wall, after which the horizontal forces can be improved by modifying the hollow core slab wall structure or by adding diagonal bracing or tensile reinforcement to the exterior.

Acknowledgments

The work was supported by National Natural Science Foundation of China Youth Science Foundation Project (52108207), Key Scientific Research Projects of Colleges and Universities in Henan Province (24A560002) and Key Scientific and Technological Projects of Henan Province (252102320296).

References

1. Li Y, Li Z, Tang Z, et al. Cyclic behavior of hollow-core precast shear walls subjected to different axial loads[J]. *Engineering Structures*, 2023, 276: 115343.
2. WANG Hongxin, SUN Zhanqi, YUAN Jijia, et al. Research on the application of prestressed hollow core slabs in high-rise buildings[J]. *Building Structure*, 2022, 52(S1): 1725-1731. DOI: 10.19701/j.jzjg.22S1581.
3. Singhal, Shubham, et al. "Behaviour of Precast Reinforced Concrete Structural Wall Systems Subjected to In-Plane Lateral Loads." *Engineering Structures* 241 (2021): 112474.
4. Zhang Weijing, Yang Leigang, Qian Jiaru, Ma Tao, Zhang Yingbao, Zhang Yuzhao. Experimental study on seismic performance of precast hollow slab shear wall with large shear span ratio [J]. *Journal of Civil Engineering*, 2019, 52 (06) : 1-13. DOI : 10.15951 / j.tmgxb.2019.06.00.
5. N. Krishna Raju. 《Principles of Prestressed Concrete》. New York; John Wiley & Sons, 1968.
6. Luo P, Liu J. An experimental study of the mechanical behaviour of squat shear walls built with precast concrete two-way hollow slabs[J]. *Journal of the South african institution of civil engineering*, 2022, 64(2): 56-66.
7. Enterprise standard of Henan Qingshui Construction Technology Co. EPP prestressed concrete hollow core slab QB/QSKJ.001-2021[S]. Henan Qingshui Construction Technology Co., Ltd, 2021.
8. Li Y, Li Z, Tang Z, et al. Cyclic behavior of hollow-core precast shear walls subjected to different axial loads[J]. *Engineering Structures*, 2023, 276: 115343.

Open Access This chapter is licensed under the terms of the Creative Commons Attribution-NonCommercial 4.0 International License (<http://creativecommons.org/licenses/by-nc/4.0/>), which permits any noncommercial use, sharing, adaptation, distribution and reproduction in any medium or format, as long as you give appropriate credit to the original author(s) and the source, provide a link to the Creative Commons license and indicate if changes were made.

The images or other third party material in this chapter are included in the chapter's Creative Commons license, unless indicated otherwise in a credit line to the material. If material is not included in the chapter's Creative Commons license and your intended use is not permitted by statutory regulation or exceeds the permitted use, you will need to obtain permission directly from the copyright holder.

